Published in final edited form as:
*Neurobiol Dis*. 2008 December ; 32(3): 391–401. doi:10.1016/j.nbd.2008.07.023.

# Functional consequences of hippocampal neuronal ectopia in the apolipoprotein E receptor-2 knockout mouse

**Kenneth. N. Fish**[1] and **Thomas Krucker**[2]

[1] Department of Psychiatry, University of Pittsburgh School of Medicine, Pittsburgh, Pennsylvania 15213

[2] Novartis Institutes for BioMedical Research, Inc. Cambridge, Massachusetts 02139

## Abstract

Little is known about the impact ectopically located neurons have on the functional connectivity of local circuits. The ApoER2 knockout mouse has subtle cytoarchitectural disruptions, altered prepulse inhibition, and memory abnormalities. We evaluated this mouse mutant as a model to study the role ectopic neurons play in the manifestation of symptoms associated with brain diseases. We found that ectopic CA1 pyramidal and inhibitory neurons in the ApoER2 knockout hippocampus are organized into two distinct stratum pyramidale layers. *In vitro* analyses found that ApoER2 is not required for neurons to reach maturity in regards to dendritic arborization and synaptic structure density, and electrophysiological testing determined that neurons in both strata pyramidale are integrated into the hippocampal network. However, the presence of these two layers alters the spatiotemporal pattern of hippocampal activity, which may explain why ApoER2 knockout mice have selective cognitive dysfunctions that are revealed only under challenging conditions.

### Keywords

hippocampus; dendritic; development; connectivity; Reelin; ApoER2; inhibitory network

## Introduction

Several human brain diseases, such as schizophrenia, autism spectrum disorders, lissencephaly, and dyslexia are associated with altered synaptic connectivity (Mirnics et al., 2001; Selkoe, 2002). Although diseases of brain connectivity are generally associated with abnormalities in cytoarchitecture (Ayala et al., 2007), little is known about the role ectopically located neurons play in the etiology of altered connectivity. Thus, animal models with defined cytoarchitectural abnormalities are needed to study the functional consequences of neuronal ectopia on circuitry.

Transgenic and spontaneously occurring mutant mice have been extremely valuable for elucidating the roles of different proteins in neuronal development. For example, the naturally occurring mutant mouse *reeler* was used to show that a deficiency in the expression of the large extracellular matrix protein Reelin results in developmental deviations in neuronal positioning and circuitry formation in laminated brain regions (e.g. cortex and hippocampus) that are

Correspondence should be addressed to: Kenneth N. Fish, Ph.D., Department of Psychiatry, Western Psychiatric Institute and Clinic, University of Pittsburgh, Biomedical Science Tower, Room W1651, Tel: 412-648-9366; Fax: 412-624-9910, E-mail fishkn@umpc.edu.

reminiscent of those hypothesized to occur in humans with connectivity disorders, such as schizophrenia and autism (D'Arcangelo et al., 1995; Fatemi et al., 2001; Howell et al., 1997; Ogawa et al., 1995; Sheldon et al., 1997). Unfortunately, similar to the functional deletion of other proteins essential for neuronal development, deletion of Reelin results in severe neuronal cytoarchitectural changes making *reeler* an unrealistic model system to study altered brain connectivity. However, subtle disruption in neuronal cytoarchitecture can be achieved by functional attenuation of essential proteins, heterozygosis of essential genes, or by knocking out genes that play minor roles in neuronal development.

An animal model in which subtle cytoarchitectural disruptions occur is the apolipoprotein E receptor-2 (ApoER2) knockout mouse. ApoER2 is a receptor for Reelin, and the transmission of the Reelin-signal via this receptor and/or the very-low-density lipoprotein receptor (VLDLR) to the cytoplasmic adaptor protein disabled-1 (Dab1) during neuronal migration is required for the establishment of normal brain architecture (Sheldon et al., 1997; Trommsdorff et al., 1999). Although brain development in ApoER2 and VLDLR double receptor knockout mice is indistinguishable from that found in the *reeler* mouse (Trommsdorff et al., 1999), in ApoER2 knockout mice ectopic neurons are found mostly in the hippocampus, while in VLDLR mutants the neuroarchitecture of the cerebellum is mostly altered (Trommsdorff et al., 1999). Thus, the distinct neuroanatomical phenotypes associated with the individual receptor knockouts suggest their functions and/or brain expression patterns only partially overlap.

ApoER2 knockout mice have been recently found to have deficits in certain aspects of prepulse inhibition that mirror those in psychotic disorders (Barr et al., 2007a). In addition, they have complex deficits in memory (Barr et al., 2007b; Dowell et al., 2004; Weeber et al., 2002) and deficits in CA1 hippocampal long-term potentiation (LTP) (Weeber et al., 2002). These findings taken together with those reporting the loose packing of neurons in CA1 of the ApoER2 knockout pyramidal layer (Trommsdorff et al., 1999) suggest that the hippocampus of the ApoER2 knockout mouse is a good candidate model system for studying the functional consequences of neuronal ectopia on local circuitry.

To assess local circuitry in ApoER2 knockout mice we have performed a thorough electrophysiological assessment of its hippocampal CA1. Our results show that ectopic neurons integrate into the hippocampal network, altering the temporal and spatial tone of inhibition. Our model suggests that these changes may contribute to the behavioral deficits these animals have in sensory motor gating and memory.

## Materials and Methods

### Antibodies and Immunostaining

Mouse anti-parvalbumin (1:1000), rabbit anti-calretinin (1:1000), mouse anti-synaptophysin (1 μg/ml) and rabbit anti-MAP2 (1:1000) antibodies were purchased from Millipore (Billerica, MA). The rabbit anti-Dab1 antibody was kindly provided by Dr. Jonathan Cooper (Fred Hutchinson Cancer Research Center, Seattle, WA). Primary and secondary antibodies were incubated for 45 minutes (dissociated cultures) or overnight (tissue sections). Species specific secondary antibodies conjugated to Alexa Fluor fluorophores were purchased from Invitrogen. NeuroTrace fluorescent Nissl stain and fluorescently conjugated phalloidin were purchased from Invitrogen (Carlsbad, CA) and used per the manufacturer's recommendations. Tissue sections, tissue slices, and dissociated cultures were mounted using Fluormount-G purchased from Electron Microscopy Sciences (Hatfield, PA).

## Animals

ApoER2 knockout (B6;129S-Lrp8$^{tm1Her}$), VLDLR knockout (B6;129S7-Vldlr$^{tm1Her}$), *reeler* mice (B6C3Fe *ala-Reln*$^{rl}$/+), and wild type (wt; B6129SF2/J) mice were obtained from The Jackson Laboratory (JAX; Bar Harbor, ME). For all studies, Littermates of ApoER2 het/VLDLR het breeders were the source of ApoER2 knockout, ApoER2 knockout/VLDLR knockout, and wt mice. In addition, mice of the same genotype used in the histological and electrophysiology experiments were from different litters. Colony maintenance was performed using dietary information provided by JAX and when necessary, wt mice of the same background (also from JAX). Genotyping was performed by PCR using protocols provided by JAX. Animal care was in accordance with institutional and NIH guidelines.

## Dissociated Cultures

Neurons were cultured at low density from embryonic day (E) 15 control and mutant mice as previously described (Aridor et al., 2004; MacLaurin et al., 2007). Briefly, hippocampal neurons were plated onto poly-L-lysine-coated glass coverslips that are inverted over a monolayer of glial cells after 2 hr incubation. Cells were plated at a density of 2700 cells per $cm^2$ to achieve low-density cultures, which were required in order to accurately measure individual dendritic branch lengths. Importantly, several precautions were taken to ensure that we had highly pure cultures of hippocampal pyramidal neurons for our study. Neurons were isolated from E15 embryos to decrease the possibility of contaminating cultures with dentate granule cells. Paraffin dots attached to the coverslips were used to keep the neurons separated from the cells making up the glial feeder. Furthermore, since the quality of the glial feeder layer, which supplies neurotrophic substances, determines how well the neurons differentiate, the feeder layer used in all experiments was generated at least one week prior to the day of the experiment from the cortices of P1 wt pups. Using glial cells derived from wt animals assured that neurons in all experiments developed in a similar environment. Most neurons, >90%, developed the characteristic mature morphology of spiny neurons between 16–21 days *in vitro* (DIV). As a measure of culture maturity in experiments using 20 DIV neurons we confirmed that the majority of the cells in the wt culture had a relatively high density of dendritic spines (0.5–1.5 punctae/μm of dendrite) using rhodamine-phalloidin.

## Microscopy

Images were collected on an Olympus FV500 confocal microscope or an Olympus IX-70 microscope (Olympus America Inc., Melville, NY) equipped with a Hamamatsu C4742–98 CCD camera (Hamamatsu Corporation, Bridgewater, NJ) and a Ludl motorized XYZ stage (LEP Ltd., Hawthorne, NY). Data was deconvolved using the Agard/Sadat inverse matrix algorithm.

To quantify dendritic characteristics 5 sequential confocal slices taken 0.1 μm apart through the midplane of the dendrites were collected with fixed laser illumination and pinhole size using a 60× 1.4 NA plan apochromat objective or a 40× 1.3 plan fluorite objective on an Olympus FV500 confocal. Using SlideBook 4.1 Imaging software (Intelligent Imaging Innovations, Inc; Denver, CO) three-dimensional images were constructed of each dendrite. The reconstructed images were then delineated and the threshold set. The number, size, and signal intensity was then measured. No significant difference was detectable in the grayscale values for each voxel within the area of interest in any of the cells or any of the conditions. Using the program ImageJ with the semiautomatic neurite tracing plugin NeuronJ (Meijering et al., 2004) we measured dendritic length based on threshold segmentation. Using these experimental parameters, the dendrites from a minimum of 21 neurons from at least three different experiments per condition were measured.

### Electrophysiology

P80–P120 mice were used for electrophysiology experiments. Our detailed methods described previously (Krucker et al., 2002; Krucker et al., 1998) were slightly modified. Briefly, mice were anesthetized with 3% halothane and decapitated. Brains were rapidly removed and immersed in ice-cold artificial cerebrospinal fluid (ACSF) containing (in mM): NaCl, 130; KCl, 3.5; KH2PO4, 1.25; MgSO4, 1.5; CaCl2, 2.0; NaHCO3 24 and glucose 10; with a pH of 7.4 and saturated with carbogen (95% O2 + 5% CO2). We dissected both hippocampi and cut transverse slices (400 μm thick) using a McIlwain tissue chopper. All experiments were done at 32 ± 0.2°C in a submerged-type slice chamber. Stimulation was delivered as indicated by square current pulses of 0.05 ms duration at 0.02 Hz through an isolated tungsten bipolar monocentric electrode. We recorded compound field potentials with glass electrodes (tip resistance 1–4 MΩ) filled with 3M NaCl and positioned either two electrodes simultaneously in cell layers or made consecutive recordings moving one electrode along a parallel line to the dendrosomatic axis of the stratum pyramidale. The evoked responses were recorded, amplified (Axoclamp-2A or -2B, Axon Instruments, Foster City, CA), digitized at a sampling rate of 10 kHz, and stored on a PC using pClamp software (Axon Instruments, Foster City, CA). We measured the pEPSP amplitude as the y-axis difference between its most negative and/or positive peak and the baseline value 1 ms preceding the stimulation; the slope was calculated as the initial negative linear segment of the trace using least-squares regression analyses. We calculated PS amplitude as the difference between two positive and the most negative peaks of the trace. We evoked PPF by delivering two stimuli of the same intensity separated by inter-pulse intervals (IPIs) as indicated. The ratio of the slopes of fEPSP2/fEPSP1 was an index of PPF. For PPI we evoked maximal somatic PS amplitude using SI approximately 2–3 times higher than for maximum pEPSP used to generate the maximal dendritic pEPSP. PPI was compared at IPIs as indicated and we calculated the ratio of the PS amplitude PS2/PS1 as the index of PPI.

### Statistical Analyses

Unless stated otherwise, one-way analysis of variance with post-hoc comparison via Tukey's Honestly Significant Difference was used to evaluate between group differences. In cases where preliminary analysis of dendritic length revealed this measure to be highly skewed, lengths were first transformed by taking their natural logarithm (ln) prior to statistical analysis. In all cases, diagnostic statistics were used to confirm that the data (actual or ln transformed) were normally distributed. In electrophysiology experiments we tested for statistically significant differences using the Mann-Whitney *U* test and considered $p < 0.05$ statistically significant.

## Results

### The cytoarchitecture of the ApoER2 knockout hippocampus

The scattering of ectopic neurons in the CA1 region of the stratum pyramidale (SP) is one of the architectural abnormalities that result from genetically disrupting the ApoER2 gene (Trommsdorff et al., 1999). To date, cytoarchitectural analyses in the literature have only described this scattering in sagittal sections. Thus, in order to determine the extent of neuronal ectopia in the SP region of the ApoER2 knockout mouse we performed a histological analysis using coronal, sagittal, and transverse slices. Coronal sections stained with fluorescent Nissl revealed two very distinct layers of neurons extending throughout the entire SP (Fig. 1B–C), which was confirmed with transverse slices (Figs. 3B and 4). Depending on the orientation and position of hippocampal sections, some of the CA3 pyramidal neurons align with the infrapyramidal blade of the dentate gyrus (Figs. 1B–D and 3B). In addition, the neuronal positioning in the entorhinal cortex (EC) results in a layered appearance (Fig. 1B).

To identify the ectopic layer of neurons we subdivided the region in CA1 that extends from the top of the stratum oriens (SO) to the stratum lacunosum-moleculare (SLM) into 10 equal sections (Supplemental Fig. 1). This was done in order to directly compare the relative position of the supra-SP (the layer closest to the alveus) and infra-SP (the neuronal layer that is farthest from the alveus) to that of a wt SP. In addition, we measured the distances between each neuronal layer and the alveus and/or the fissure in both coronal and sagittal hippocampal sections. We found that in more caudal coronal sections (Fig. 1B) and sagittal sections (Fig. 1D) the infra-SP lies within the stratum radiatum (SR), approximately 100 μm closer to the fissure than the SP of wt hippocampi. However, we also discovered that the supra-SP lies within what would be the wt SO. An analysis of serial coronal brain sections revealed that the number of neurons in the supra-SP increases when moving rostral to caudal along the rostrocaudal axis (Fig. 1B–C). Since previous studies have shown that a substantial number of hippocampal pyramidal neurons of *reeler* mice are misoriented (Niu et al., 2004; Stanfield and Cowan, 1979), we used an antibody against MAP2 to determine the orientation of neurons in both of the ApoER2 knockout strata pyramidale. Fig. 1F–H demonstrate that the majority of neurons in both strata pyramidale are oriented such that their apical dendrites point towards the SR, which is similar to what is found in wt hippocampi (Fig. 1E). The positioning of the two ApoER2 knockout strata pyramidale in relation to a wt SP are summarized in Figure 7.

The abnormalities in ApoER2 hippocampal cytoarchitecture suggest that the majority of SP neurons require ApoER2 to receive the Reelin signal. To quantitatively test this possibility we determined the number of hippocampal pyramidal neurons *in vitro* that are unable to effectively receive the Reelin signal in ApoER2 knockout mice using the expression level of Dab1 as a determinant of a neuron's ability to transmit the Reelin signal across the plasma membrane (PM) (Hiesberger et al., 1999; MacLaurin et al., 2007; Rice et al., 1998). For these studies we used levels of Dab1 expression rather than antibodies directed against ApoER2 and VLDLR for several reasons. For example, using single knockout animals, we have not been able to convincingly demonstrate the specificity of commercially available antibodies directed against ApoER2 or VLDLR. In addition, even if we had a VLDLR specific antibody, the level of VLDLR expression in some neurons may be below the detection limits of our system, resulting in falsely classifying neurons as ApoER2 negative/VLDLR negative when they actually express VLDLR. In order to define the meaning of being a Reelin responder or non-responder using Dab1 expression we first used quantitative immunofluorescence microscopy to determine the somatic expression levels of Dab1 in 3 DIV and mature (18–20 DIV) wt (n=20 and 18, respectively) and ApoER2 knockout/VLDLR knockout (n=18 at both stages of differentiation) neurons (Supplemental Fig. 2). Although, we have previously shown that Reelin is expressed in the culture supernatant and that approximately 9–12% of the neurons in our hippocampal neuron cultures express Reelin (MacLaurin et al., 2007), for all *in vitro* experiments we added recombinant Reelin to the culture media to ensure that all neurons had equal access to Reelin as previously described (MacLaurin et al., 2007). At 3 DIV the somatic expression of Dab1 in neurons from ApoER2 knockout/VLDLR knockout cultures was more than 3 fold greater than in wt neurons [138.67 (STDEV=25.30) versus 40.51 (STDEV=23.65), respectively]. By the time they reached maturity, ApoER2 knockout/VLDLR knockout neurons expressed almost five times more somatic Dab1 than mature wt neurons [180.31 (STDEV=17.67) versus 36.33 (STDEV=17.33), respectively]. Using the Dab1 expression values determined for neurons from ApoER2 knockout/VLDLR knockout and wt cultures we classified neurons in ApoER2 knockout cultures as either being a Reelin responder or non-responder in the following manner. Reelin responders were considered to be a neuron that expressed less Dab1 than the mean expression level of Dab1 in wt controls plus 2 STDEV (3 DIV) or 2.5 STDEV (mature). Reelin non-responders were classified as expressing more Dab1 than the mean ApoER2 knockout/VLDLR knockout Dab1 expression level minus 2 STDEV (3 DIV) or 2.5 STDEV (mature). Importantly, using these criteria all neurons in our wt and ApoER2 knockout/VLDLR knockout cultures were correctly classified. We next randomly

imaged 27 3 DIV and 25 mature neurons from ApoER2 knockout cultures and determined the average mean intensity of Dab1 in their somas in order to classify them as being Reelin responders or non-responders. All cells imaged at the 3 DIV time point fell into one of the two categories: 13 responders and 14 non-responders (Supplemental Fig. 2). Thus, greater than 50 percent of neurons imaged did not appropriately downregulate Dab1 expression in response to Reelin. Although similar ratios between the number of responders and non-responders (11 and 11, respectively) were found in mature ApoER2 knockout cultures, 3 out of 25 neurons imaged were unclassifiable under the current criteria (Supplemental Fig. 2).

## ApoER2 and VLDLR are not required for dendrites to fully elongate *in vitro*

We have recently shown that Dab1 is not required for neurons to reach maturity with respect to dendritic length and complexity (MacLaurin et al., 2007). However, it is unknown if ApoER2 or VLDLR are required for neurons to reach a similar level of maturity. Therefore, to determine if ApoER2 is required for neurons to reach maturity *in vitro* we performed a microscopic examination of dendritic processes in neuronal cultures derived from wt and ApoER2 knockout/VLDLR knockout embryos at 4, 7, and 20 DIV. We chose to assess cultures derived from ApoER2 knockout/VLDLR knockout embryos rather than those derived from ApoER2 knockout embryos because it was the most efficient way to determine if hippocampal neurons are dependent on ApoER2 for reaching maturation since all neurons in the culture could be assessed. Our quantitative analysis was performed using high magnification images of isolated neurons from three or more different cultures from each genotype (Fig. 2A–C). At 4 DIV dendrites in the ApoER2 knockout/VLDLR knockout cultures were significantly shorter than those in wt cultures, which could be detected at both the average dendrite length ($p<0.005$; Fig. 2C) and total dendritic length per neuron ($p<0.01$; Supplemental Fig. 3A). However, there were no statistically significant differences in either measurement of dendritic length at 7 or 20 DIV (Fig. 2C and Supplemental Fig. 3A). Although these findings are similar to those in the study that compared wt and Dab1 knockout cultures (MacLaurin et al., 2007), unlike the previous study we also detected significant differences in primary ($p<0.001$) and secondary ($p<0.001$) dendritic branch lengths between wt and ApoER2 knockout/VLDLR knockout cultures at 4 DIV (Supplemental Fig. 3B). Additional analyses of dendritic development found no significant differences between ApoER2 knockout/VLDLR knockout and wt cultures in the total number of dendrites and the number of dendrites that had secondary and tertiary branches at 4, 7, and 20 DIV (Supplemental Fig. 3E). Thus, similar to neurons that lack Dab1, neurons derived from ApoER2 knockout/VLDLR knockout embryos have only modest deficits in the rate at which dendrites develop at very early stages of development that are no longer present by 7 DIV.

## Synaptic structural markers in neuronal cultures derived from ApoER2 knockout/VLDLR knockout embryos

Although we have shown that neurons that cannot receive the Reelin-Dab1 signal are able to reach maturity with respect to dendritic elongation and complexity, it is unknown if these neurons make synaptic connections *in vitro*. Therefore, we analyzed the staining pattern of presynaptic and postsynaptic markers of neurons derived from wt, ApoER2 knockout, and ApoER2 knockout/VLDLR knockout mouse embryos. Punctate staining of the presynaptic marker synaptophysin was detected along the dendrites of mature neurons derived from all 3 genotypes (Fig. 2F–H). Similarly, dendritic spines were visualized on dendrites using phalloidin (Fig. 2D–E) and an antibody against PSD95 (postsynaptic density protein 95; Fig. 2I). Quantitative analyses of spine (PSD-95) and presynaptic cluster (synaptophysin) densities found no significant differences between mature wt and ApoER2 knockout/VLDLR knockout neurons (Fig. 2J). Taken together, the above findings suggest that primary hippocampal neurons derived ApoER2 knockout embryos would reach maturity *in vitro* in regards to dendritic arborization and synaptic structure density.

## Ectopic pyramidal hippocampal neurons in ApoER2 knockout mice are integrated into the local circuitry

To test whether neurons in the CA1 region of ApoER2 knockout are receiving input from Schaeffer collaterals (SC) and are functionally integrated in the hippocampal network, we used electrophysiological techniques to perform a laminar profile analysis of electrically evoked field potentials. Consecutive recordings along the dendrosomatic axis of the pyramidal cell layer produced laminar profiles of field potentials evoked by stimulation of SC in SR (Fig. 3). In slices from wt mice, this type of electrical stimulation evoked a long-duration negative going population excitatory postsynaptic potential (pEPSP) with maximal amplitude in the mid distal apical dendritic region of pyramidal cells (traces 10–12, Fig. 3A). The pEPSP negativity declined in amplitude with proximity to the SP and inverted to a positive polarity in the region of the cell body layer (traces 3–6). The maximal amplitude of the positivity was found in SP or the proximal-mid SO, regions corresponding to the level of somata and proximal basal dendrites of pyramidal cells. In the region of the cell body layer, stimulation evoked a sharp negative population spike (pSp) upon the positive going synaptic potential (Fig. 3A, trace 5, and Fig. 5C3). The largest-amplitude and shortest-latency pSp was found in the region of the SP. Within basal and apical dendritic regions the pSps were usually absent. Occasionally, the polarity of the pSp inverted in SR to a biphasic negative/positive potential, overlaying the negative going pEPSP.

In slices from ApoER2 knockout mice laminar profiles of pEPSPs were similar to wt with the maximal negative amplitude in the mid distal apical dendritic region of pyramidal cells (Fig. 3B, traces 10–12). However, rather than having one single peak like in wt slices, amplitudes of positive going pEPSPs (in the region of the two strata pyramidale) were more evenly distributed. These positive going pEPSPs were characterized by prolonged duration and multiple, although smaller, negative going spikes, both typical for polysynaptic pEPSPs (Fig. 3B, traces 2–4). Laminar profiles of pSp in ApoER2 knockout slices were significantly different from wt (Fig. 3 and Fig. 4). Whereas in wt slices, the profile of the pSp amplitude displayed one single peak in the region of the SP, we found two distinct peaks in ApoER2 knockout slices. The average amplitude of the supra-SP pSp was about 80% of the infra-SP pSp. However, changing the position of the stimulation electrode to the area in between the two strata pyramidale reversed this relationship so that the average amplitude of the supra-SP pSp was now about 140% of the infra-SP pSp. The two distinct peaks of the pSp amplitude profile suggest that both strata pyramidale are integrated in the hippocampal circuitry, receiving synaptic input from SC. The obvious differences in the laminar profile of field potentials suggest that the current density source function in the CA1 region of ApoER2 knockout mice is also altered.

As a comparison we determined laminar profiles in slices from *reeler* mice. A typical example is shown in Fig. 3 and Fig. 4. In contrast to wt and ApoER2 knockout, SC stimulation evoked dominant-negative going pSp responses upon positive pEPSPs throughout the slice reflecting the absence of a clearly defined SP (also see (Bliss and Chung, 1974;Ishida et al., 1994)).

## Paired-pulse facilitation of pEPSP in ApoER2 knockout mice is normal

Paired-pulse facilitation (PPF) of the pEPSP, a test designed to determine changes in presynaptic neurotransmitter release remained unaltered at all intervals tested in ApoER2 knockout slices when compared to slices from wt littermate controls (Fig. 5A–B). Generally, the PPF ratio has an inverse relationship to the neurotransmitter release probability. Thus, the unaltered PPF suggests that presynaptic calcium homeostasis and glutamate release are intact in ApoER2 knockout slices.

### Paired-pulse inhibition is decreased in the infra-SP and increased in the supra-SP

To test the function of inhibitory feed-forward and feed-back neurons, and to estimate the integrity of gamma-aminobutyric acid (GABA) inhibitory interneurons within CA1 of wt and ApoER2 knockout slices, we used a paired-pulse protocol of the pSp. Paired-pulse inhibition (PPI) was evoked with superthreshold stimulation intensities and measured at 10, 20, 50, 100, and 200 ms in both strata pyramidale simultaneously. In wt slices, the inhibition of the second pSp was most obvious at interpulse intervals (IPIs) of 10 ms (Fig. 6A). During simultaneous recordings from both strata pyramidale in slices from ApoER2 knockout mice, stimulation of SR induced a significant increase of inhibition in the supra-SP at 10, 20, and 50 ms IPIs compared to wt slices. However, in the infra-SP PPI was significantly reduced at all IPIs tested (Fig. 6A–B). Moving the stimulation electrode to in between the strata pyramidale increased PPI of the infra-SP to levels of wt, but did not change PPI of the supra-SP (Fig. 6C–D). These results prove that the inhibitory neurons in the CA1 region of ApoER2 knockout slices are functional. However, the significant differences of PPI between the supra-SP and infra-SP suggest that there is altered connectivity.

### Inhibitory neurons are mispositioned along with pyramidal neurons

Our findings that PPI is significantly decreased in the infra-SP and significantly increased in the supra-SP of slices from ApoER2 knockout mice suggest that the local inhibitory system is, to some extent, intact in both these layers. Therefore, we performed an immunohistochemical analysis of the positioning of inhibitory neurons in the hippocampus of ApoER2 knockout mice. Experiments using antibodies against calcium binding proteins found that parvalbumin-reactive and calretinin-reactive neurons are scattered among the pyramidal neurons of the supra-SP and infra-SP (Fig. 7). The patterning of calretinin-reactive neurons in ApoER2 knockout mice was qualitatively similar to that in wt mice (Fig. 7 and data not shown). However, we found a substantially greater number of parvalbumin positive neurons in the ApoER2 knockout SR compared to wt (Fig. 7 and data not shown). The increase in parvalbumin-immunoreactive neurons in the SR is likely a result of the migration of theses neurons to associate with pyramidal neurons of the infra-SP.

## Discussion

Neuronal mispositioning during development may contribute to altered brain connectivity associated with psychiatric and neurological disorders (Lewis and Levitt, 2002). The cytoarchitectural changes in the hippocampus pyramidal layer of the ApoER2 knockout mouse makes this mouse a good model to study the functional consequences that ectopic neurons have on local circuitry. Electrophysiological studies presented here found that the spatiotemporal pattern of hippocampal activity is altered in ApoER2 knockout mice. Together with data from our thorough evaluation of ApoER2's role in neuronal maturation and hippocampal cytoarchitecture, the present findings may help explain why ApoER2 knockout mice have selective cognitive dysfunctions that are revealed only under challenging conditions (Barr et al., 2007a; Barr et al., 2007b; Dowell et al., 2004; Weeber et al., 2002).

### ApoER2 deletion splits SP neurons into two distinct layers

Our cytoarchitectural findings extend previous reports that analyzed the neuronal ectopia in the SP of ApoER2 knockout mice using sagittal brain sections (Drakew et al., 2002; Trommsdorff et al., 1999; Weeber et al., 2002). Specifically, the neurons forming the SP are divided into two distinct layers (supra-SP and infra-SP). Surprisingly, neither the infra-SP's or the supra-SP's position matches that of a wt SP (Supplemental Fig. 1). A possible explanation for this finding would be that Reelin signaling through VLDLR alone in SP pyramidal neurons is incapable of transmitting enough Reelin-Dab1 signal to facilitate positioning. In caudal slices infra-SP and supra-SP layers appear to consist of equal numbers of neurons and both extend

from CA3 through the fissure into the EC (Fig. 1B). However, serial coronal and sagittal brain sections revealed that the number of neurons in the supra-SP varies drastically along the rostrocaudal axis (Fig. 1B–D). Given that a rostrocaudal gradient of hippocampal involvement has been suggested to play an integral part in complex psychiatric disorders (Csernansky et al., 2002; Heckers, 2001), the ApoER2 knockout mouse may be helpful in understanding aspects of the neuropathology that result in abnormal brain connectivity associated with autism, schizophrenia, and epilepsies.

### The role(s) of ApoER2 and VLDLR in dendritic maturation

Using a primary neuronal culture system that supports the full maturation of neurons we recently showed that neurons deficient in Dab1 signaling developed mature dendrites in respect to length and complexity. However, their initial tempo of dendritic elongation was slowed compared to wt neurons (MacLaurin et al., 2007). Similarly, we have shown here that neurons incapable of receiving the Reelin signal via ApoER2 and VLDLR are able to reach maturity *in vitro* in regards to dendritic length, dendritic complexity, and synaptic cluster density (Fig. 2). In addition, neurons derived from ApoER2 knockout/VLDLR knockout embryos also have altered initial kinetics of dendritic development. The hippocampus develops in a very sequential time dependent manner (Caviness, 1973; Grove and Tole, 1999; Heimrich et al., 2002). The correct positioning of neurons and their rate of development during this process are key to the establishment of connectivity with specific target cells. Thus, although the altered local connectivity described here is most likely the consequence of the ApoER2 knockout hippocampal cytoarchitecture, one cannot rule out that the altered tempo of earlydendrite development, if present *in vivo*, may play a role.

### CA1 laminar profiles in ApoER2 knockout mice reflect the presence of the supra-SP and infra-SP

Although we have shown that the changes in hippocampal architecture associated with ApoER2 deficiency are severe, the local hippocampal environment permits the survival of ectopic SP neurons that appear to have their apical dendrites pointing towards the stratum radiatum. Therefore, we assumed that the neurons in both the supra-SP and infra-SP receive input from the Schaeffer collaterals and functionally integrate into the synaptic network of the hippocampus. In support of this idea, field potentials recorded along the ApoER2 knockout dendrosomatic axis resembled those of wt (Fig. 3). However, CA1 laminar profiles are distinctively different from wt (Fig. 4) suggesting that connectivity is altered.

The actual site of pSp as the final output following integration of excitatory and inhibitory synaptic potentials is of paramount importance for information processing within the brain circuitry. The distinct CA1 laminar profiles that result from ApoER2 deficiency alter the current source density, which directly modulates the excitability of pyramidal neurons because of the ability of the EPSP to evoke an action potential is changed, a process known as EPSP to spike coupling (Lu et al., 2000; Magee, 2000). These changes in excitability are most likely a result of the attenuation of inhibitory inputs (Chavez-Noriega et al., 1989). Therefore, we suggest that feed-forward and/or feed-back inhibitory input suppresses action potential firing and regulates synaptic development and plasticity through a subpopulation of interneurons in the CA1 region of ApoER2 knockout mice. In support of this view, we determined that PPF is unchanged in ApoER2 knockout slices, which is in accordance with the findings of Weeber and colleagues (Weeber et al., 2002).

### Altered inhibition in the ApoER2 knockout hippocampus

We found that PPI is significantly decreased in the infra-SP and significantly increased in the supra-SP of slices from ApoER2 knockout mice. In fact, PPI is reversed to PPF of the pSp in the infra-SP, suggesting reduced inhibitory tone, either through a reduced number of inhibitory

cells or synaptic connections. Because antidromic stimulation of the infra-SP, which was performed by placing the stimulating electrode between the supra-SP and infra-SP (Fig. 6C), increased PPI to wt levels, the local inhibition in the infra-SP appears to be intact. However, we cannot exclude the possibility that the position of our stimulation electrode excites neurons of the supra-SP, which in turn generates additional local inhibition, adding to the inhibitory tone of the infra-SP (see Fig. 7).

Through a complex mechanism inhibitory cells influence pyramidal cell excitability and network functioning in the brain (Nakajima et al., 1991). In the ApoER2 knockout hippocampus this complexity is amplified because the patterning of parvalbumin-immunoreactive neurons is drastically altered compared to wt (Fig. 7). The altered positioning of parvalbumin-immunoreactive neurons in the SR is most likely the result of the migration of these neurons to associate with pyramidal neurons of the infra-SP (Ishida et al., 1994). One consequence of this reorganization may be that feedback inhibitory neurons synapsing onto pyramidal neurons within the supra-SP receive considerable additional input from infra-SP excitatory neurons. This altered spatial inhibitory tone presumably would influence synchronization mechanisms like gamma and theta rhythms, affecting exploration, arousal, rapid eye movement sleep, plasticity, and memory storage (Banks et al., 2000). Such changes may also influence the induction of long-term potentiation (LTP), which would explain the deficits in LTP Weeber and colleagues found in ApoER2 knockout mice (Weeber et al., 2002). These findings support the use of the ApoER2 knockout mouse as a model for neuronal ectopia in neurological and neuropsychiatric disorders.

## Altered hippocampal circuitry and topology in ApoER2 knockout mice may explain complex behavior

Our findings show that ectopic neurons in the ApoER2 knockout hippocampus integrating into the intrinsic tri-synaptic circuitry. Amazingly, the adaptation to neuronal ectopia in the ApoER2 knockout mouse is sufficient to sustain normal baseline behavioral activity. Specifically, when behavior relies largely on intra-hippocampal synaptic connectivity (e.g. memory retention), wt and knockout mice behavior is equivalent (Barr et al., 2007b). Surprisingly, ApoER2 knockout mice have significantly greater cross-modal prepulse inhibition (Barr et al., 2007a) and they appear to use more sophisticated search strategies when navigating the Barnes circular maze (Barr et al., 2007b). Thus, in some instances when the hippocampus is required to integrate into the larger network of the brain there is actually an enhancement in the functional output.

Developmentally, altered brain connectivity can result from the convergence of genetic predispositions and environmental factors that affect neuronal positioning and/or function. Indeed, in the ApoER2 knockout mouse adaptations most likely intended to sustain certain behaviors appear to come at a cost, reflected partially as a loss of behavioral flexibility in response to stressors (Barr et al., 2007a; Barr et al., 2007b). Specifically, ApoER2 knockout mice performed significantly worse on a memory reversal task in our previous Barnes maze study (Barr et al., 2007b). In addition, in another study when ApoER2 knockout mice were challenged with the NMDA receptor antagonist PCP, which induces schizophrenia-like symptoms in healthy volunteers and exacerbates symptoms in schizophrenia patients (Luby et al., 1959), they were significantly more sensitive to the cognitive-disruptive effects of the drug (Barr et al., 2007a). Furthermore, ApoER2 knockout mice have been found to have contextual fear conditioning deficits (Weeber et al., 2002) and to display poorer memory retention on the Morris water maze (Dowell et al., 2004).

In conclusion, our studies combined with those that reported ApoER2 deficient mice have altered behavioral phenotypes (Barr et al., 2007a; Barr et al., 2007b; Dowell et al., 2004; Weeber et al., 2002) suggest that the ApoER2 knockout intra-hippocampal circuitry allows

these mice to function normally in hippocampal-dependent tasks when demands on this system are moderate. However, under challenging conditions, such as during stress or encounter with environmental perturbations, there are selective dysfunctions in ApoER2 knockout mice. With that said, ApoER2 deficiency itself may also play a role in their etiology.

## Supplementary Material

Refer to Web version on PubMed Central for supplementary material.

## Acknowledgments

We are grateful to Drs. David Lewis, Athina Markou, Rob Sweet, and Jonathan Cooper for their constructive comments, and to Amy Guzik and Sarah MacLaurin for technical assistance and advice. This work was supported by a NARSAD Young Investigator Award and NIMH (MH064372) grant to KNF.

## References

Aridor M, et al. Endoplasmic reticulum export site formation and function in dendrites. J Neurosci 2004;24:3770–6. [PubMed: 15084657]

Ayala R, et al. Trekking across the brain: the journey of neuronal migration. Cell 2007;128:29–43. [PubMed: 17218253]

Banks MI, et al. Interactions between distinct GABA(A) circuits in hippocampus. Neuron 2000;25:449–57. [PubMed: 10719898]

Barr AM, et al. The reelin receptors VLDLR and ApoER2 regulate sensorimotor gating in mice. Neuropharmacology. 2007a

Barr AM, et al. Altered performance of reelin-receptor ApoER2 deficient mice on spatial tasks using the Barnes maze. Behav Neurosci 2007b;121:1101–5. [PubMed: 17907841]

Bliss TV, Chung SH. An electrophysiological study of the hippocampus of the ‘reeler’ mutant mouse. Nature 1974;252:153–5. [PubMed: 4421774]

Caviness VS Jr. Time of neuron origin in the hippocampus and dentate gyrus of normal and reeler mutant mice: an autoradiographic analysis. J Comp Neurol 1973;151:113–20. [PubMed: 4744470]

Chavez-Noriega LE, et al. The EPSP-spike (E-S) component of long-term potentiation in the rat hippocampal slice is modulated by GABAergic but not cholinergic mechanisms. Neurosci Lett 1989;104:58–64. [PubMed: 2554222]

Csernansky JG, et al. Hippocampal deformities in schizophrenia characterized by high dimensional brain mapping. Am J Psychiatry 2002;159:2000–6. [PubMed: 12450948]

D’Arcangelo G, et al. A protein related to extracellular matrix proteins deleted in the mouse mutant reeler [see comments]. Nature 1995;374:719–23. [PubMed: 7715726]

Dowell KK, et al. Differential splicing of ApoER2 is involved in Reelin signaling and modulation of NMDA receptors. Soc Neurosci Abstr 2004;843:12.

Drakew A, et al. Dentate granule cells in reeler mutants and VLDLR and ApoER2 knockout mice. Exp Neurol 2002;176:12–24. [PubMed: 12093079]

Fatemi SH, et al. Dysregulation of Reelin and Bcl-2 proteins in autistic cerebellum. J Autism Dev Disord 2001;31:529–35. [PubMed: 11814262]

Grove EA, Tole S. Patterning events and specification signals in the developing hippocampus. Cereb Cortex 1999;9:551–61. [PubMed: 10498273]

Heckers S. Neuroimaging studies of the hippocampus in schizophrenia. Hippocampus 2001;11:520–8. [PubMed: 11732705]

Heimrich B, et al. Axon guidance and the formation of specific connections in the hippocampus. Neuroembryology 2002;1:154–160.

Hiesberger T, et al. Direct binding of Reelin to VLDL receptor and ApoE receptor 2 induces tyrosine phosphorylation of disabled-1 and modulates tau phosphorylation. Neuron 1999;24:481–9. [PubMed: 10571241]

Howell BW, et al. Neuronal position in the developing brain is regulated by mouse disabled-1 [see comments]. Nature 1997;389:733–7. [PubMed: 9338785]

Ishida A, et al. An electrophysiological and immunohistochemical study of the hippocampus of the reeler mutant mouse. Brain Res 1994;662:60–8. [PubMed: 7859091]

Krucker T, et al. Targeted disruption of RC3 reveals a calmodulin-based mechanism for regulating metaplasticity in the hippocampus. J Neurosci 2002;22:5525–35. [PubMed: 12097504]

Krucker T, et al. Transgenic mice with cerebral expression of human immunodeficiency virus type-1 coat protein gp120 show divergent changes in short- and long-term potentiation in CA1 hippocampus. Neuroscience 1998;83:691–700. [PubMed: 9483553]

Lewis DA, Levitt P. Schizophrenia as a disorder of neurodevelopment. Annu Rev Neurosci 2002;25:409–32. [PubMed: 12052915]

Lu YM, et al. Calcineurin-mediated LTD of GABAergic inhibition underlies the increased excitability of CA1 neurons associated with LTP. Neuron 2000;26:197–205. [PubMed: 10798404]

Luby ED, et al. Study of a new schizophrenomimetic drug; sernyl. AMA Arch Neurol Psychiatry 1959;81:363–9.

MacLaurin SA, et al. Hippocampal dendritic arbor growth in vitro: Regulation by Reelin-ApoER2/VLDLR-Dab1 signaling in a dose- and time-dependent manner. J Neurosci. 2007

Magee JC. Dendritic integration of excitatory synaptic input. Nat Rev Neurosci 2000;1:181–90. [PubMed: 11257906]

Meijering E, et al. Design and validation of a tool for neurite tracing and analysis in fluorescence microscopy images. Cytometry 2004;58A:167–76. [PubMed: 15057970]

Mirnics K, et al. Analysis of complex brain disorders with gene expression microarrays: schizophrenia as a disease of the synapse. Trends Neurosci 2001;24:479–86. [PubMed: 11476888]

Nakajima S, et al. Local circuit synaptic interactions between CA1 pyramidal cells and interneurons in the kainate-lesioned hyperexcitable hippocampus. Hippocampus 1991;1:67–78. [PubMed: 1669343]

Niu S, et al. Reelin Promotes Hippocampal Dendrite Development through the VLDLR/ApoER2-Dab1 Pathway. Neuron 2004;41:71–84. [PubMed: 14715136]

Ogawa M, et al. The reeler gene-associated antigen on Cajal-Retzius neurons is a crucial molecule for laminar organization of cortical neurons. Neuron 1995;14:899–912. [PubMed: 7748558]

Rice DS, et al. Disabled-1 acts downstream of Reelin in a signaling pathway that controls laminar organization in the mammalian brain. Development 1998;125:3719–29. [PubMed: 9716537]

Selkoe DJ. Alzheimer's disease is a synaptic failure. Science 2002;298:789–91. [PubMed: 12399581]

Sheldon M, et al. Scrambler and yotari disrupt the disabled gene and produce a reeler- like phenotype in mice [see comments]. Nature 1997;389:730–3. [PubMed: 9338784]

Stanfield BB, Cowan WM. The morphology of the hippocampus and dentate gyrus in normal and reeler mice. J Comp Neurol 1979;185:393–422. [PubMed: 438366]

Trommsdorff M, et al. Reeler/Disabled-like disruption of neuronal migration in knockout mice lacking the VLDL receptor and ApoE receptor 2. Cell 1999;97:689–701. [PubMed: 10380922]

Weeber EJ, et al. Reelin and ApoE receptors cooperate to enhance hippocampal synaptic plasticity and learning. J Biol Chem 2002;277:39944–52. [PubMed: 12167620]


**Figure 1. Hippocampal cytoarchitectural changes in the SP of ApoER2 knockout mice**

Coronal (A–C) and sagittal (D) sections of P80 wild type (wt; A) and ApoER2 knockout (ko; B–D) hippocampi were processed for immunocytochemistry using a fluorescent Nissl stain. Moving rostral (C) to caudal (B) the double layering of the SP in hippocampus becomes much more pronounced extending from CA3 to the entorhinal cortex. In B the circle marks the alveus and the square the fissure. Also in B, the supra-SP and infra-SP are labeled. (E–H) Coronal sections of P80 wt (E) and ApoER2 ko (F–H) hippocampi were processed for immunocytochemistry using a fluorescent Nissl stain (red) and an antibody directed towards MAP2 (green). (G–H) Higher magnifications of the ApoER2 ko CA1 supra-SP (G) and infra-

SP (H). Arrows point to apical dendrites. Scale bars in A = 100 μm and is also for B–D. Scale bars in E & G = 10 μm. The scale bar in E is also for F; and in G is also for H.

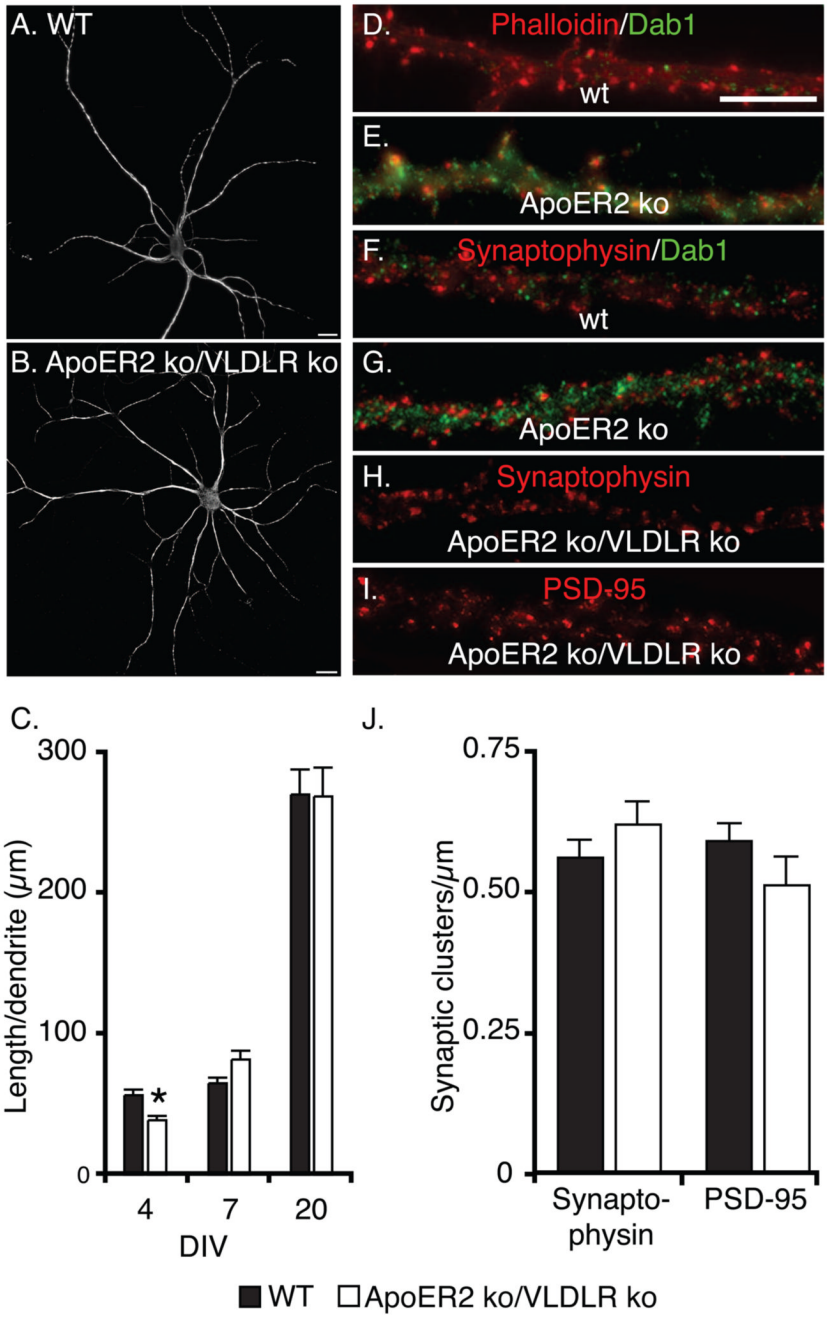


**Figure 2. ApoER2/VLDLR are not required for dendrites to reach maturity in regards to length, complexity, and synaptic cluster density *in vitro***

(A–B) MAP2 immunofluorescence of 20 DIV primary hippocampal neurons derived from wt (A) and ApoER2 knockout (ko)/VLDLR ko (B) E15 embryos. (C) Double-label immunofluorescence using a MAP2 antibody and Hoechst dye was used to quantify dendritic length in wt and ApoER2 ko/VLDLR ko neuronal cultures at 4, 7, and 20 DIV. (D–I) Immunofluorescence analysis of mature primary hippocampal neurons derived from wt (D and F), ApoER2 ko (E and G), and ApoER2 ko/VLDLR ko (H–I) E15 mouse embryos. (D–E) Double-label immunofluorescence using an antibody directed towards Dab1 (green) and fluorescently conjugated phalloidin (red). (F–G) Double-label immunofluorescence using

antibodies directed towards Dab1 (green) and synaptophysin (red). (H–I) Synaptophysin (red; H) and PSD95 (red; I) staining of mature neurons derived from ApoER2 ko/VLDLR ko E15 embryos. (J) A quantitative comparison of synaptic clusters in wt and ApoER2 ko/VLDLR ko cultures. Scale bars in A–B equal 20μm, while the bar in D is also for E–I and equals 10 μm. In C and J values equal mean ± SEM and the asterisk in C designates a significant difference from wt.

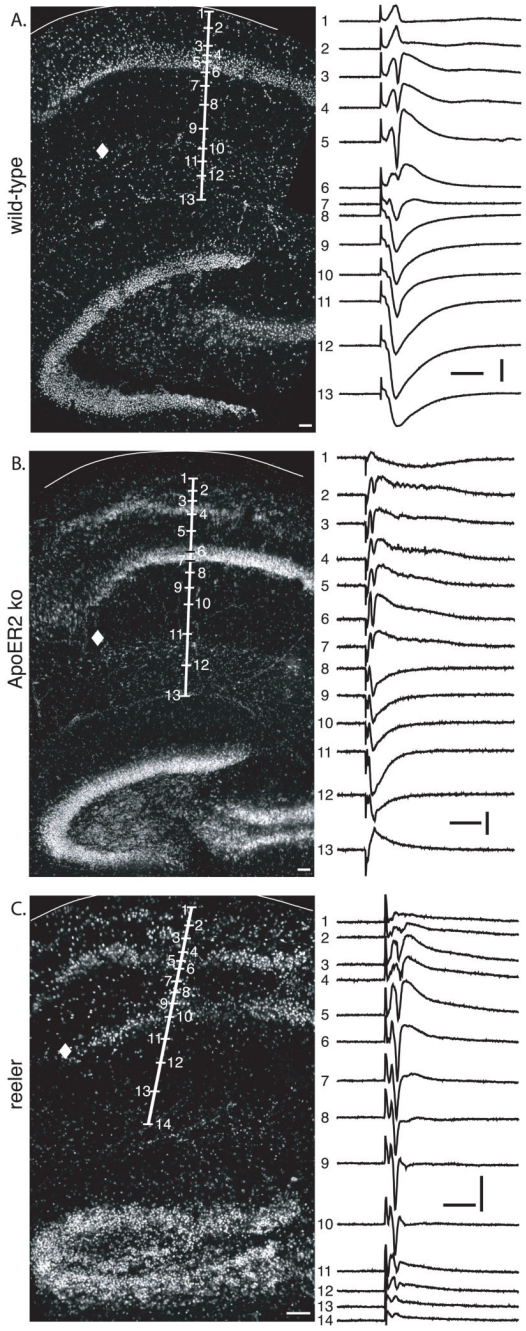


**Figure 3. Representative laminar profiles of field potentials in CA1 of hippocampal slices**

Original traces (right panels) are actual recordings from (A) wt, (B) ApoER2 knockout (ko), and (C) *reeler* slices depicted on the left. Following suprathreshold SC stimulation in SR we made consecutive field potential recordings parallel to the dendrosomatic axis of the SP. (A) In wt slices (representative of 12 slices from 4 mice) SC stimulation evoked long-duration negative going population pEPSP (#7–#13) with maximal amplitude in the mid-distal apical dendritic region of pyramidal cells (trace #11) which was inverted to a positive polarity in the region of the cell body layer and proximal-mid SO (#1–#6). A sharp negative pSp upon the positive going synaptic potential appeared in the region of the cell body layer (#3–#6), but was absent in the basal and apical dendritic regions (#7–#13). (B) In slices from ApoER2 ko mice

(representative of 13 slices from 4 mice) SC stimulation evoked pEPSPs similar to wt animals with the maximal negative amplitude in the mid distal apical dendritic region of pyramidal cells (#11). Amplitudes of positive going pEPSPs in the region of the two strata pyramidale (#1–#7) were more evenly distributed. Note the prolonged duration and multiple negative going sSPs on all the positive pEPSPs. (C) In *reeler* mice (representative of 6 slices from 2 mice), SC stimulation evoked dominant-negative going pSp responses upon positive pEPSPs throughout the slice (#1–#14) reflecting the absence of a clearly defined cell body layer. In A–C the diamond symbol indicates the position of the stimulation electrode. Calibration bars: horizontal: 10 ms, vertical 1 mV. All scale bars equal 50 μm.

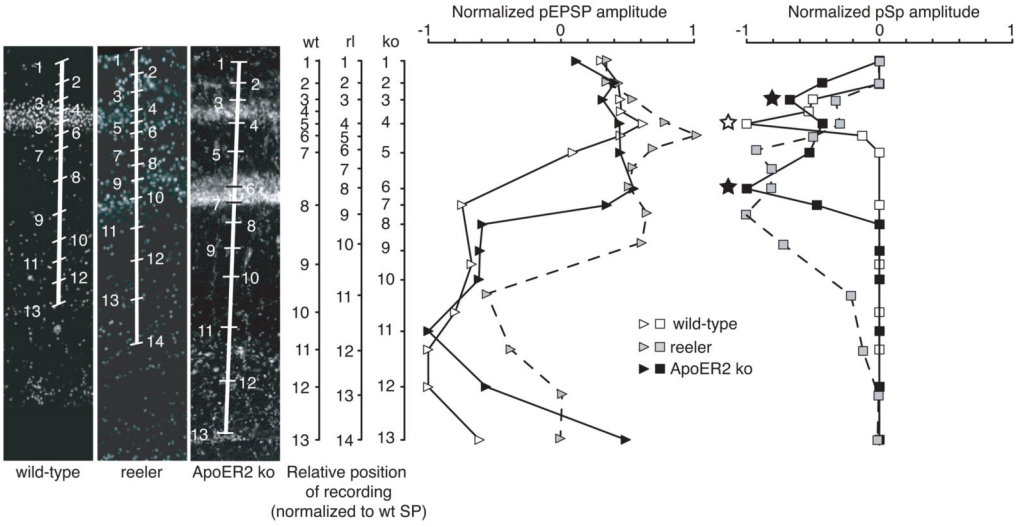


**Figure 4. Laminar profiles of normalized pEPSP and pSp in CA1 of hippocampal slices from ApoER2 wt, knockout, and *reeler* mice**

Left panels show recording locations within respective slices (size adjusted). X-axis is calculated as relative pEPSP (left graph) or pSp (right graph) amplitude at the specific recording locations. Y-axis represents recording location as normalized distance to the center of the SP and/or supra-SP. In slices from wt mice (representative of 12 slices from 4 mice) the pEPSP with maximal amplitude is in the mid distal apical dendritic region of pyramidal cells. The maximal amplitude of the positivity in the SP steadily declines through the SO, a region corresponding to the proximal based dendrites of pyramidal cells. In slices from ApoER2 knockout (ko) mice (representative of 13 slices from 4 mice) laminar profiles of negative going pEPSPs resemble wt profiles, however, positive going pEPSPs (in the region of the two strata pyramidale) are more evenly distributed, rather than having one single peak like in wt slices. A typical profile of the pSp in ApoER2 ko displays two distinct peaks (black stars) instead of one (white star) as in wt slices. The largest-amplitude is found in the region of SP in wt slices. In both, wt and ApoER2 ko slices, pSps are absent within basal and apical dendritic regions. In ApoER2 ko slices, the average amplitude of the smaller pSp closer to SO (supra-SP) is about 80% of the larger pSp (closer to SR, infra-SP). Surprisingly, the largest pEPSP amplitude in *reeler* mice (representative of 6 slices from 2 mice) is positive going and is in the area where a wt SP would be located. Significant negative going pSps are already present, what usually corresponds to the mid distal dendritic region of pyramidal cells in a wt slice. Such a profile reflects the absence of clearly defined SP.

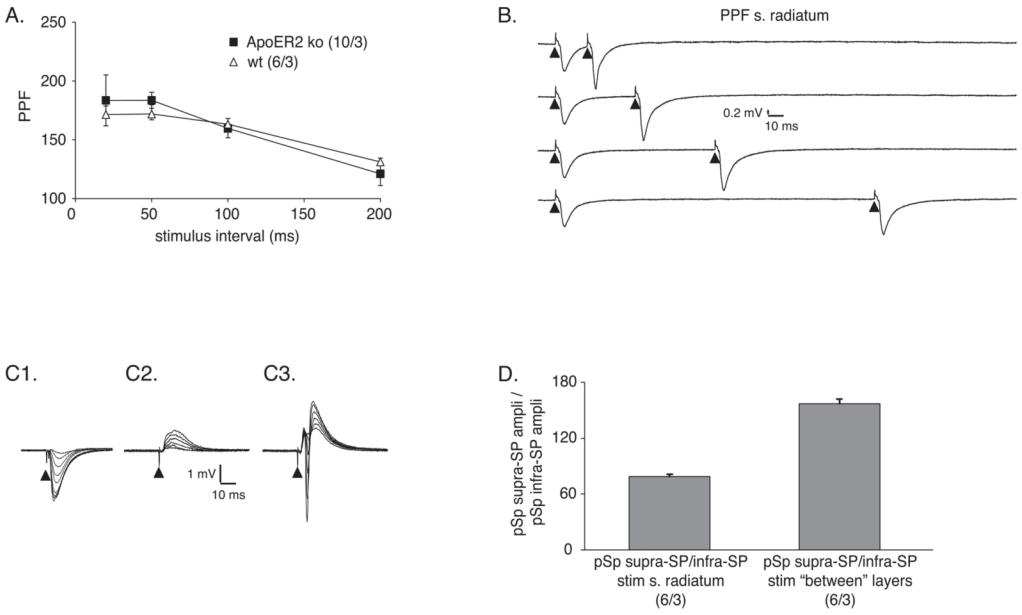


**Figure 5. PPF in CA1 of ApoER2 knockout mice**

(A) PPF of the dendritic pEPSP at different interstimulus intervals is normal in CA1 of ApoER2 knockout (ko) slices. (B) Traces showing typical PPF at different stimulation intervals. The primed (second) pEPSP after 20, 50, 100 and 200 ms is larger than the first one, representing the facilitation. Arrowheads below these and following traces indicate the artifacts from electrical stimulation. (C) Representative traces from negative going dendritic pEPSPs (C1) recorded in SR, positive going somatic pEPSP (C2) and pSp (C3), both recorded in SP, after gradual increase of SC stimulation in a wt slice. (D) The ratio of the average maximal pSps of the infra-SP and the supra-SP reverses after the stimulation electrode is moved in between the layers. SR stimulation evokes larger pSps in the infra-SP and in between layer stimulation evokes larger pSp in the supra-SP. [N=(number of slices/number of mice)]

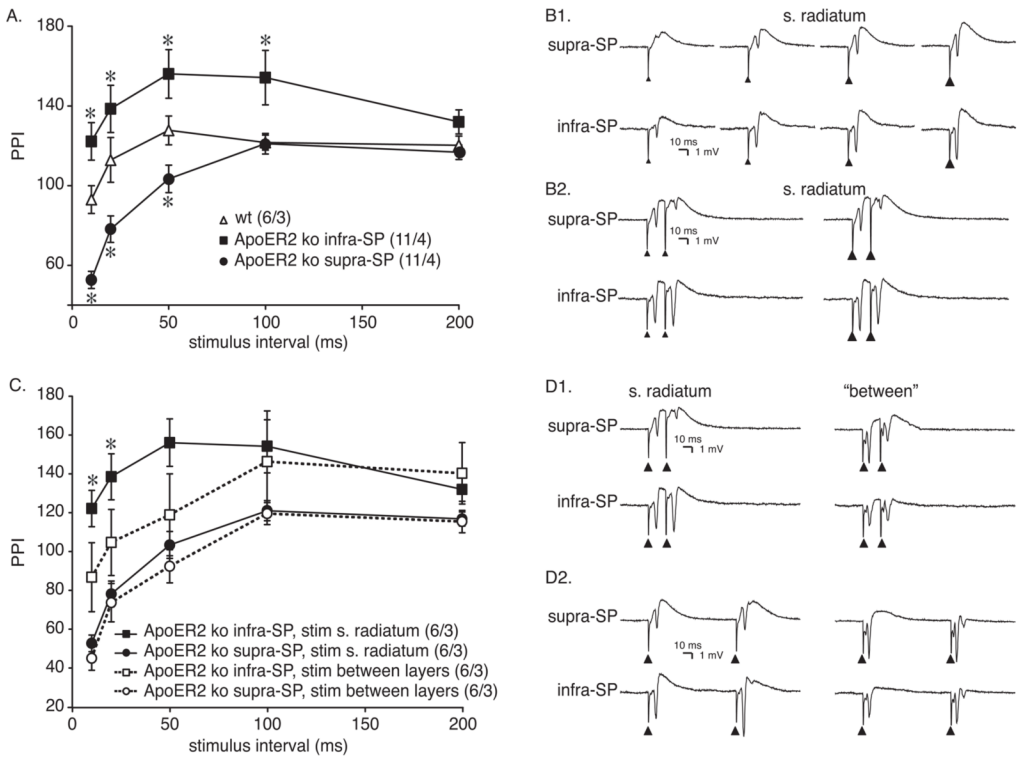


**Figure 6. PPI in CA1 of ApoER2 knockout mice**

(A) Simultaneous recordings in supra-SP and infra-SP show that SC paired stimulation evokes increased PPI of pSp in the supra-SP and facilitation of pSp (reduced PPI) in the infra-SP compared to wt. (B1) Traces of pSps recorded in supra-SP and infra-SP. Increasing stimulation intensities indicated by increasing size of arrowheads, evoke gradually larger pSps. Averaged maximal pSps in the infra-SP are larger than in the supra-SP (also see Fig. 5D). (B2) Representative traces of PPI at 10 ms interval. At maximal stimulation, in the supra-SP paired-pulse stimulation evokes strong inhibition of the second pSp, whereas in the infra-SP the second pSp is clearly larger (facilitated). Increasing SC stimulation intensity (larger arrowheads) further increases the inhibition in the supra-SP and slightly reducing the facilitation in infra-SP. (C) Moving the stimulation electrode in between the two strata pyramidale reverses the facilitation of the pSp in the infra-SP into PPI similar to wt. PPI in the supra-SP remains the same as when the stimulation electrode is in the SR. (D) Single traces of PPI at 10 (D1) and 50 (D2) ms interval at supra-maximal stimulation. In the infra-SP PPF changes to PPI but PPI in the supra-SP remains unchanged. In A and C the data points are shown with SEM and the asterisks designate a significant difference from wt. [N=(number of slices/number of mice)]

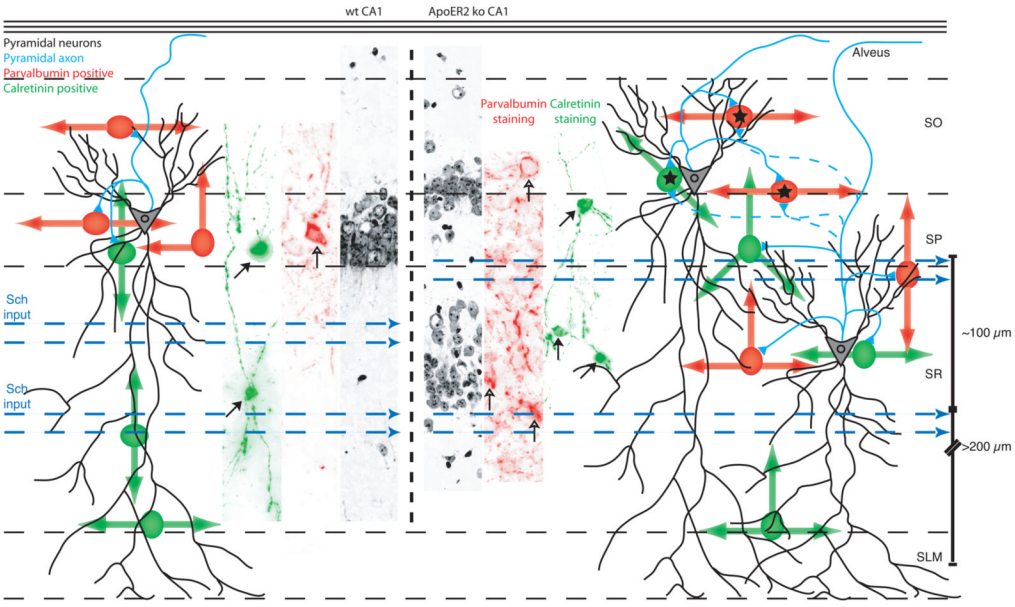


**Figure 7. Connectivity and interneuron distribution in the CA1 of the ApoER2 knockout hippocampus**

Using data from the present study and from experiments designed to localize inhibitory neurons in the hippocampus of wt and knockout (ko) mice we have modeled the CA1 regions of these animals. The positioning of pyramidal neurons (grey) is presented as IF images taken of Nissl stained slices. The locations of parvalbumin positive (red) and calretinin positive (green) neurons were detected by IF. To determine both the location of their soma and the orientation of their projections we used serial hippocampal slice sections and antibodies directed towards these calcium-binding proteins. IF microscopy images of representative slices are inserted. Parvalbumin and calretinin positive somas are designated with open and filled arrows, respectively. The direction of the major projections that express these calcium-binding proteins is depicted using arrows. Cells marked with stars represent feedback inhibitory neurons synapsing onto pyramidal neurons within the supra-SP that likely receive additional input (dashed lines) from infra-SP excitatory neurons.